AD-A266 423

MEASUREMENTS OF THE OPERATION OF THE SINUS-VI/BWO SYSTEM

Kyle J. Hendricks
Thomas A. Spencer

May 1993

Final Report

DTIC
ELECTE
JUN 23 1993
S
E
D

93-13991

93 6 23 019

PL-TR--93-1003

This final report was prepared by the Phillips Laboratory, Kirtland Air Force Base, New Mexico, under Job Order 5797AK04. The Laboratory Project Officer-in-Charge was Dr. Kyle J. Hendricks (WSR).

When Government drawings, specifications, or other data are used for any purpose other than in connection with a definitely Government-related procurement, the United States Government incurs no responsibility or any obligation whatsoever. The fact that the Government may have formulated or in any way supplied the said drawings, specifications, or other data, is not to be regarded by implication, or otherwise in any manner construed, as licensing the holder, or any other person or corporation; or as conveying any rights or permission to manufacture, use, or sell any patented invention that may in any way be related thereto.
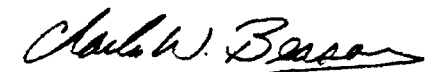
This report has been authored by an employee of the United States Government. Accordingly, the United States Government retains a nonexclusive royalty-free license to publish or reproduce the material contained herein, or allow others to do so, for the United States Government purposes.

This report has been reviewed by the Public Affairs Office and is releasable to the National Technical Information Service (NTIS). At NTIS, it will be available to the general public, including foreign nationals.
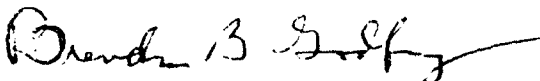
If your address has changed, or if you wish to be removed from the mailing list, please notify PL/WSR, 3550 Aberdeen Ave SE, Kirtland AFB, NM 87117-5776 to help us maintain a current mailing list.

This report has been reviewed and is approved for publication.

KYLE J. HENDRICKS
Senior Physicist
Project Officer

FOR THE COMMANDER

CHARLES W. BEASON, Maj, USAF   BRENDAN B. GODFREY, ST
Chief, Electromagnetic Sources   Acting Director, Advanced Weapons
 Division   and Survivability Directorate

REPORT DOCUMENTATION PAGE

1. AGENCY USE ONLY (Leave blank)	2. REPORT DATE	3. REPORT TYPE AND DATES COVERED
	May 1993	Final, 1 Sep 92 - 1 Dec 92

4. TITLE AND SUBTITLE

MEASUREMENTS OF THE OPERATION OF THE
SINUS-VI/BWO SYSTEM

5. FUNDING NUMBERS

PE: 62601F
PR: 5797
TA: AK
WU: 04

6. AUTHOR(S)

Kyle J. Hendricks, Thomas A. Spencer

7. PERFORMING ORGANIZATION NAME(S) AND ADDRESS(ES)

Phillips Laboratory
3550 Aberdeen Avenue, SE
Kirtland AFB, NM 87117-5776

8. PERFORMING ORGANIZATION REPORT NUMBER

PL-TR--93-1003

9. SPONSORING/MONITORING AGENCY NAME(S) AND ADDRESS(ES)

10. SPONSORING MONITORING AGENCY REPORT NUMBER

11. SUPPLEMENTARY NOTES

12a. DISTRIBUTION/AVAILABILITY STATEMENT

Approved for public release; distribution is unlimited.

12b. DISTRIBUTION CODE

13. ABSTRACT (Maximum 200 words)

A series of measurements were completed on the SINUS-VI/BWO system presently located at the UNM EECE Dept. These measurements were necessary to establish that the rf and pulse power performance meet the contract specification. Measurements included antenna pattern plots, pulse power diagnostics, and calculations to establish what the microwave system should radiate. The SINUS VI pulse power device produces $V_p \sim 600$ kV, $I \sim 5$ kA, $\tau \sim 10$ ns at 200 pulses per second. The BWO parameters are P $\sim$ 500 MW, $\tau \sim 10$ ns, $\lambda \sim 3$ cm ($f \sim 10$ GHz). The slow wave structure is inserted into a segmented solenoid which produces a magnetic field of $B_z \sim 30$ kG with axial uniformity over 120 mm at a radius of 20 mm.

14. SUBJECT TERMS

high power microwave, HPM, SINUS-VI, Tesla transformer,
backward wave oscillator, BWO

15. NUMBER OF PAGES

22

16. PRICE CODE

17. SECURITY CLASSIFICATION OF REPORT	18. SECURITY CLASSIFICATION OF THIS PAGE	19. SECURITY CLASSIFICATION OF ABSTRACT	20. LIMITATION OF ABSTRACT
Unclassified	Unclassified	Unclassified	SAR

CONTENTS

Accesion For

NTIS CRA&I	☒
DTIC TAB	☐
Unannounced	☐
Justification	

By _____

Distribution /

Availability Codes

| Dist | Avail and/or Special |
| A-1 | |

FIGURES

1.0 INTRODUCTION

The Narrowband High Power Microwave source group recently purchased a SINUS-VI electron beam accelerator and a Backward Wave Oscillator (BWO) (Ref. 1) from the Russian Academy of Sciences (High Current Electronics Institute [HCEI]) through a U.S. contractor. The system was acquired because of its unique capabilities which were demonstrated in Russia and reported in the open literature (Ref. 2). The Air Force Office of Scientific Research, Wright Laboratory, and the University of New Mexico Electrical Engineering and Computer Engineering (UNM EECE) department cooperated in the acquisition. Sandia National Laboratory (SNL), Albuquerque, New Mexico has been collaborating in a computational study of the SINUS-VI/BWO system.

The experiments discussed in this document have fostered an environment which may allow U.S. scientists and engineers to gain a better understanding of Russian High Power Microwave (HPM) technology. The verification of the SINUS-VI/BWO allowed one of the first opportunities to compare Russian diagnostic techniques directly with U. S. techniques. While there are many areas of commonality between Russian and U.S. researchers, there are still areas where confusion arises. This confusion will not be eliminated until more collaborations are completed.

2.0 THE SINUS-VI SYSTEM AND PULSE POWER MEASUREMENTS

The pulse power driver (Fig. 1) may be simply viewed as an energy storage capacitor which energizes the primary of a "Tesla" Transformer (Ref. 3). Note that in this application a "Tesla" Transformer is simply a step-up transformer. The secondary of the transformer energizes a Pulse Forming Line (PFL) which establishes the pulse length and accomplishes some impedance matching to the vacuum diode. The high voltage is applied to a foilless diode. An applied external axial magnetic field is sufficient to cause the electron beam to flow axially through the vacuum electron beam line.

The pulser has various capacitative voltage probes and several I-dot (Rogowski coils or B-dot) probes incorporated into the system (Ref. 3). The probes are located on the other side of the wall shown at the left of Figure 1. Probes of these types provide derivative signals of the waveform under study (voltage or current). Typically one then uses passive integrators or numerical processing of the derivative signal to recover the representative waveform. However, in this system, because of the short time duration of the pulse, the data cable has sufficient capacitance to make the probes self-integrating. This caused confusion at first because this detail was not included in the documentation of the system. Several MICROCAP circuit simulations* established that this is the correct understanding of the diagnostic system (Figs. 2 and 3). Representative SINUS-VI diode voltage and current data are shown in Figure 4. The voltage has a rise and fall time on the order of 6 ns, and the full width at half-maximum (FWHM) is about 12 ns. The current waveform shows a slight delay in the initiation of emission, however, the FWHM is comparable to the voltage waveform.

---

*Courtesy of Jack Graham; Maxwell Laboratories, Albuquerque, New Mexico.

Figure 1. The SINUS VI pulse power system. The capacitors are located in the cabinet below the cylinder (where SINUS-6 is written) containing the Tesla Transformer.

Figure 2. The MicroCap III circuit used to simulate the SINUS-VI voltage and current pulse.

3

Figure 3. The MicroCap simulation output of the SINUS-VI pulser and voltage probe data (V = 650 kV, I = 4.5 kA).

Figure 4. The SINUS-VI voltage and current data. Peak voltage = 666 kV and peak current = 4.56 kA.

3.0 MICROWAVE CIRCUIT AND MEASUREMENTS

This microwave circuit consists of cylinders with a sinusoidally varying inner radius. There were four cylinders with different inner radii:

a) $r1(z) = 1.550 \text{ cm} + 0.100 \text{ cm} \cos(k\,z)$

b) $r2(z) = 1.515 \text{ cm} + 0.135 \text{ cm} \cos(k\,z)$

c) $r3(z) = 1.425 \text{ cm} + 0.225 \text{ cm} \cos(k\,z)$

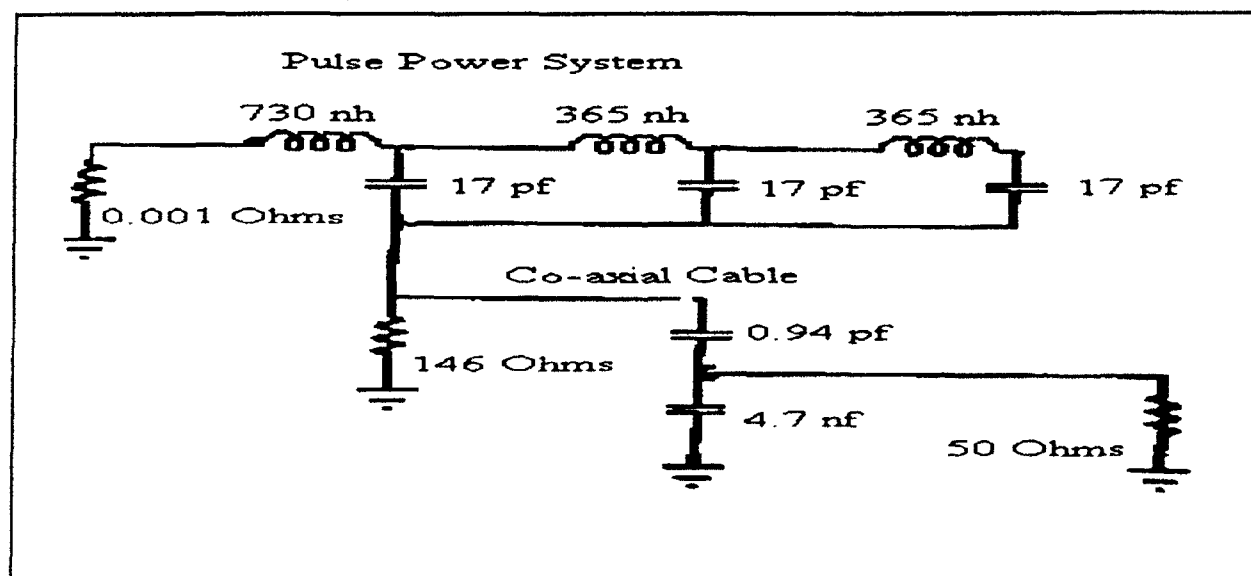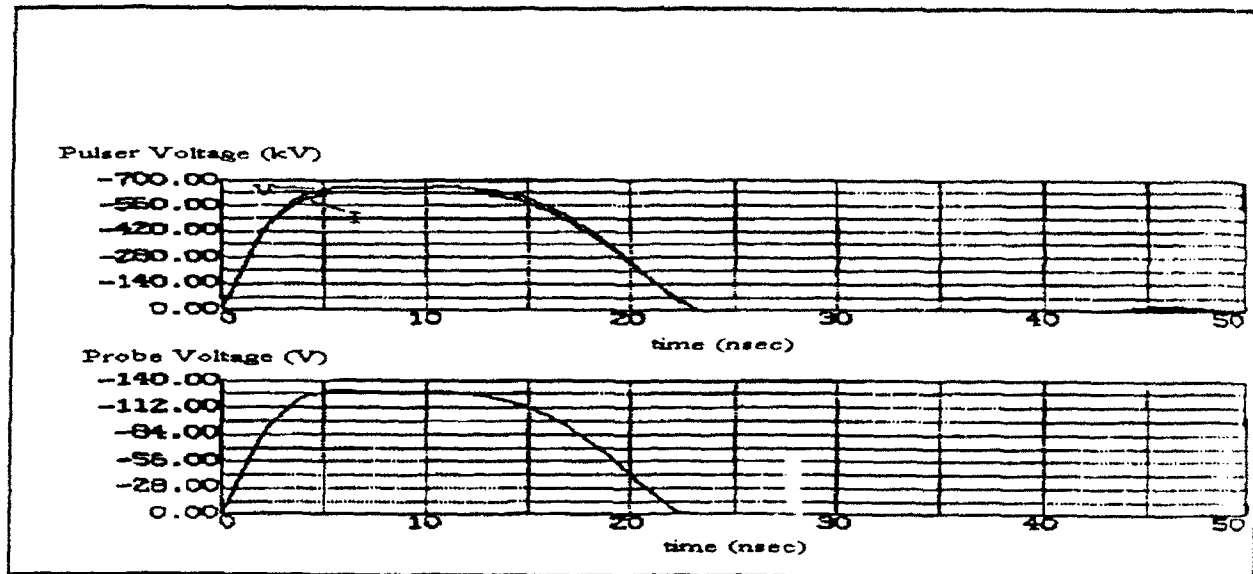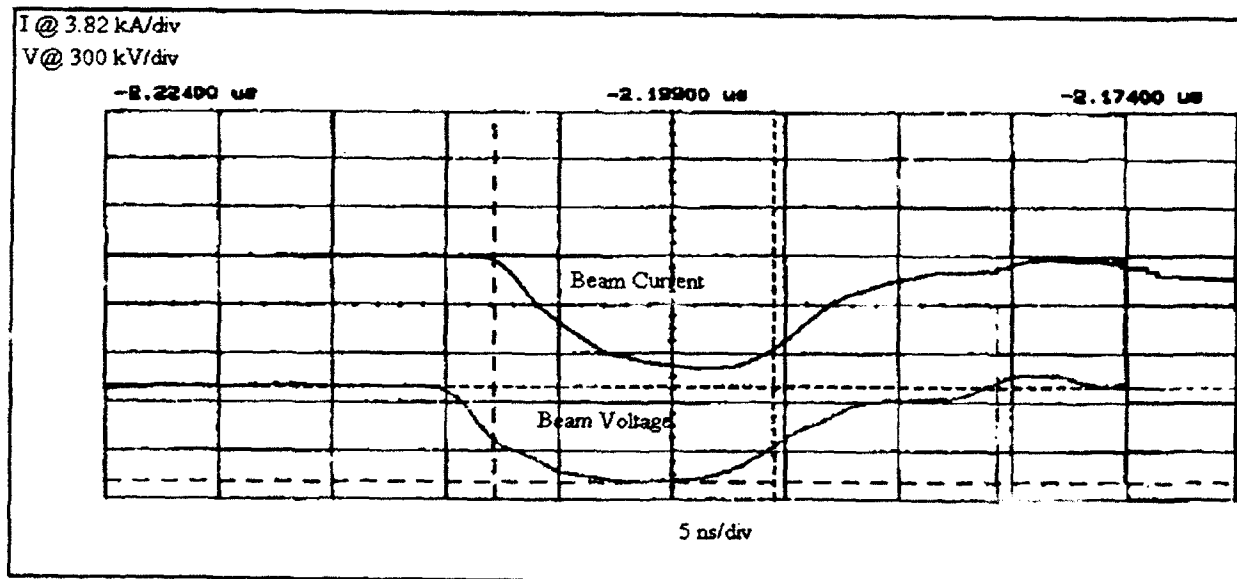d) $r4(z) = 1.400 \text{ cm} + 0.250 \text{ cm} \cos(k\,z)$

where $k = 2\pi/\lambda$, and λ is the radio frequency (rf) wavelength. These four cylindrical sections could be used in any order to form a slow wave structure; such as a uniform structure with radius $r1(z)$, or a tandem structure of initial radius $r2(z)$ and final radius $r4(z)$, or any other sequence of cylindrical sections. It should be clear that different slow wave structures may produce different frequencies. Initially, it was understood that there were two different radii used in the structure: six sections of one radius followed by six sections of a second radius. The variation in radius allows for higher efficiency by slowing down the phase velocity of the rf wave as the electron beam slows due to energy being extracted. Actually, all four cylinders were used in assembling the BWO structure (Fig. 5). Initially insertion of several electric field probes (E-dot) to monitor the microwave mode had been suggested. Due to the external magnetic field coils, and the time available for completion of the measurements this was impractical.
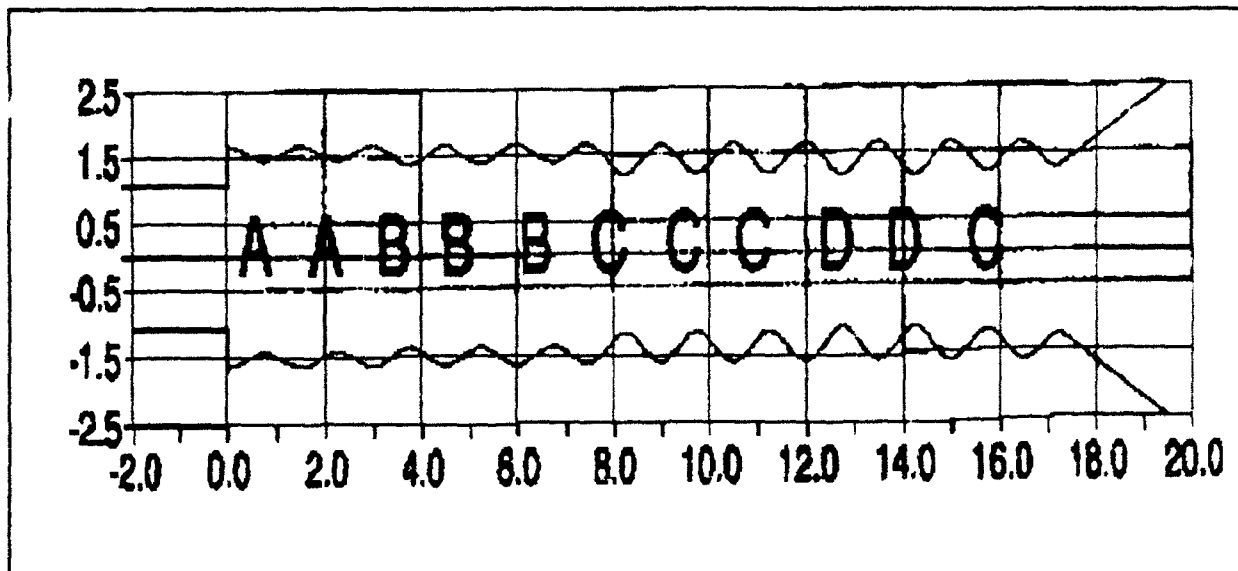
Figure 5. Diagram of the slow wave structure showing the four different radii cylinders and their position as used in the experiment. Dimensions are in cm.

4.0 RESULTS

At the time the measurements were completed, several thousand pulses had been generated and a baseline of operation had been completed by the HCEI and the UNM EECE Department. Their measurements have been presented elsewhere (Ref. 4). The pulse power system was found to be highly reliable, and the associated control equipment (timing modules, software, etc.) enabled almost a "turnkey" system. The cathode employed was a standard stainless steel cylinder. The HPM system had been tuned by the Russian scientists during installation, and the data indicated that the system met the contract specification, that is $V \sim 650$ kV, $I \sim 5$ kA, $P \sim 500$ MW.

During the first day of pulses (Pulse Nos. 1 through 35, Fig. 6) the system behaved quite reproducibly and there was little difficulty obtaining data once a probe located nearer the voltage and current monitors was used to provide a stable timing fiducial. The timing jitter in the pulse was due to a gas switch between the initial trigger probe and data probes. A scatter plot of the voltage and current for each pulse is shown in Figure 6. Notice that during pulses 1 through 30 the current follows any change in the pulser voltage almost exactly. That is, the impedance stays almost constant. The constant impedance was maintained during a modest increase in the output voltage. However, following shot 30 the pulser had a slight change in the diode impedance and a change was observed in the microwave power detected at 1.8 m from the antenna aperture. Also the diode voltage considerably exceeded the specified voltage, and that the variation was about 7 percent of the median voltage (750 kV). Fluctuation in voltage is one parameter that is typically minimized for efficient operation of BWOs. The diode current did not show the same increase observed in the voltage.

Figure 6. Scatter plots of the diode voltage and emitted current.

The variation in the diode voltage affects the strength of coupling between the electron beam and slow wave structure, therefore the efficiency of the microwave generation is also affected. This may best be understood by visualizing the efficiency as a "Gaussian-like" curve versus beam voltage. The peak efficiency is obtained at some voltage V_o; if one changes the voltage up or down intentionally or if the pulse power is not reproducible, then the efficiency will drop. Given that the pulse power initially produced a voltage pulse on the order of 650 kV to 700 kV (a $\pm$ 4% variation) seems to indicate that when the voltage increased in later shots the coupling strength was changed. The amount of change is

8

dependent on the exact shape of the coupling curve. Typically the coupling curve is maximum at some optimum set of operating parameters and then rapidly decreases from the optimum point.

The microwave measurements were accomplished with an unflanged WR-90 waveguide defining the receiver aperture. The signal was converted to a transverse electromagnetic (TEM) wave on RG-214 50-Ω cable which carried the signal to the screen room. The signal was then split for separate power and frequency diagnostics. A heterodyne technique was used to determine the difference frequency from a known oscillator frequency. Also the signal was attenuated prior to applying the TEM wave to a crystal diode detector. All filters, attenuators, crystal and cables were calibrated at 10 GHz prior to use in the experiment, and the crystal detector had a flat frequency response from 9 to 11 GHz. The diagnostic setup differed from the HCEI setup in that the HCEI diode detector was located between the coaxial cable and the waveguide receiver. The HCEI diagnostic setup precludes determining the frequency of the output radiation, which, as will be discussed later, kept some interesting data hidden.

The fundamental differences in the two diagnostic schemes are with the signal to noise ratio and the cable attenuation. The crystal provided by the HCEI provides volts per kilowatt (V/kW) of signal, and because the signal is converted from rf to video frequencies the cable loss is minimal. However, the noise environment may induce several volts of noise on the cable. The system employed here has several hundred volts of rf induced on the cable with the same lower frequency noise signal. Because the rf signal is available in the screen room, one is able to make accurate measurements of the specific frequency generated.

The rf signal was radiated from a circular aperture of a straight cylinder at the end of the antenna (Fig. 7). A curved glass window was used for a vacuum/air interface. The antenna pattern is not calculable analytically, and in fact attempting a numerical calculation proved to be intractable. The pattern observed is shown in Figure 8. The solid line is an analytical approximation to the measured data. The pattern is believed to be azimuthally
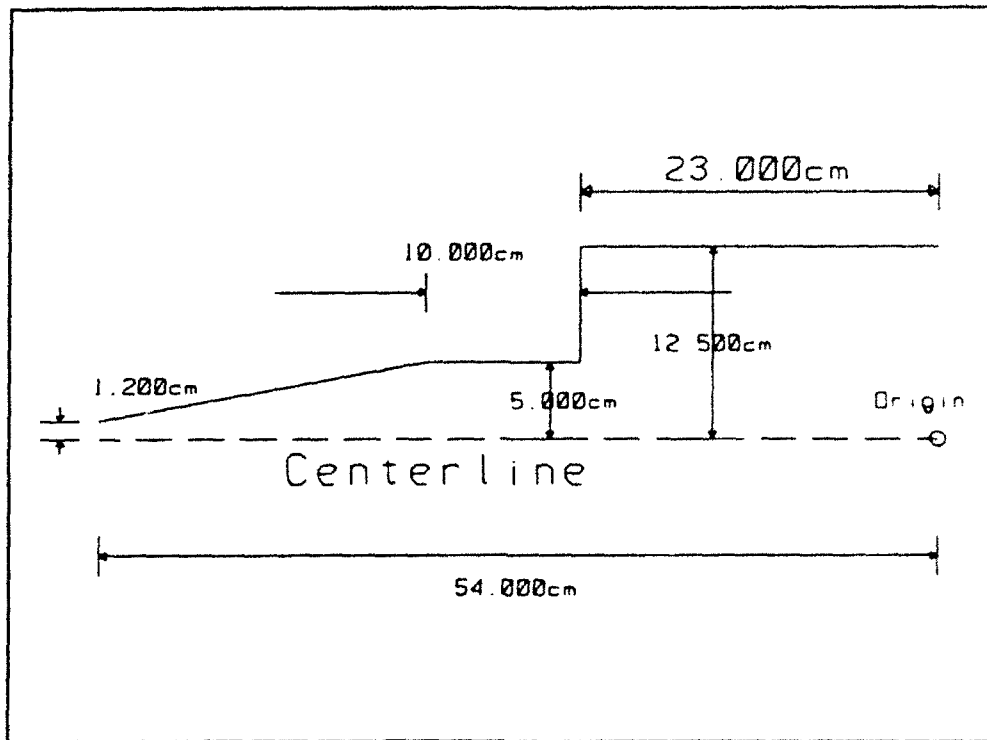
Figure 7. Diagram of radiating antenna. The origin for the power measurements is the center of the exit window.
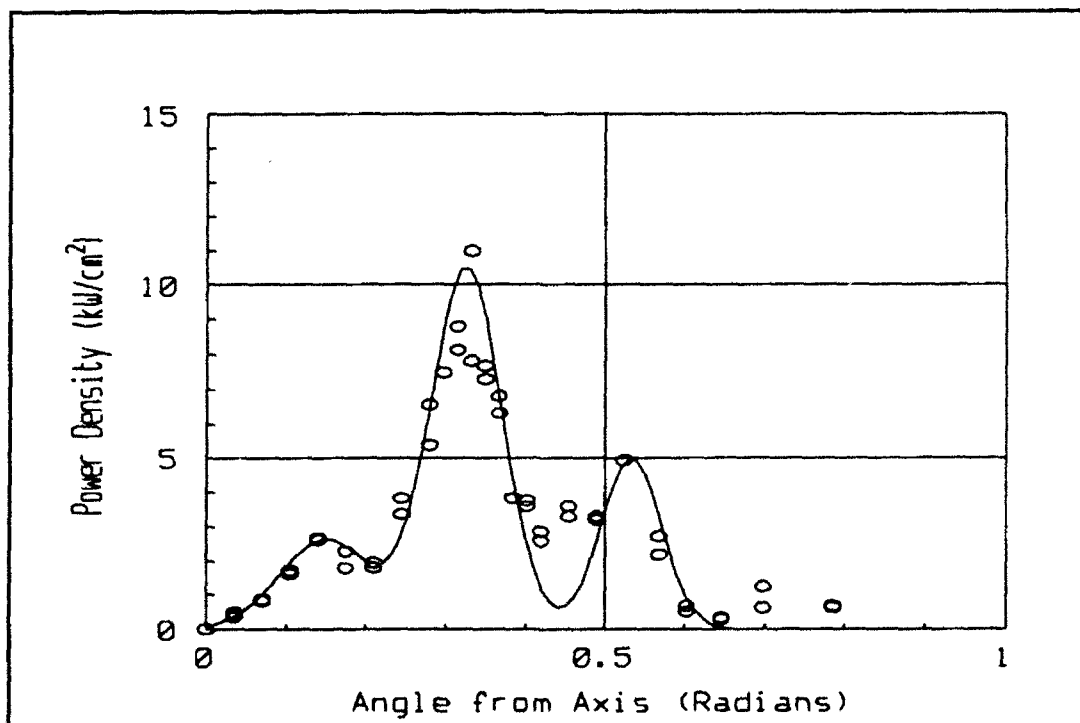

Figure 8. Antenna pattern measured from the original SINUS-VI antenna (r = 1.8 m from center of aperture).

symmetric about zero radians (the axis of the electron beam). The multiple peaks may be due to a variety of causes. One is the possibility of standing waves within the BWO/ Antenna system caused by the finite length of the slow wave structure and the step discontinuity in the radiating antenna. Another is the possibility of other frequencies or modes being generated in the BWO/Antenna system. The numerically fitted curve to the antenna map data was integrated to determine the total power radiated through the aperture. The azimuthal symmetry of the pattern was used to simplify the integral. The number determined was 270 MW, rather than 500 MW. This is attributed to the change in diode voltage noted earlier. The power received through the WR-90 aperture dropped by 3 dB when the voltage increased. The 270 MW and a 3 dB decrease translate to a radiated power >500 MW during the initial pulses. During the early measurements, that is prior to the change in voltage, the frequency was 9.6 GHz and later two different frequencies were observed to radiate from the BWO: 9.65 GHz and 10.1 GHz. Simple analytic calculations of a simple sinusoidal BWO indicate these frequencies could be due to different rf modes, or they may be due to finite length effects of the slow wave structure. In any event, the fact that another frequency was observed indicates that the monochromaticity may be sacrificed to accommodate the higher power efficiency. This cannot be determined with the present Russian setup due to where the rf wave is converted to a video signal; however, the mechanism generating these multiple frequencies must be identified to understand why this device is so efficient.

One other interesting feature of this system was the magnetic field coils. The coils were to produce a field that was uniform for about 12 cm of axial length. However, the coils are all basically identical and closely spaced. The total length of the coils is 24 cm and the BWO length is 23 cm. Therefore, based on past experience, the axial magnetic field is not constant throughout the microwave system. A calculation of the axial magnetic field based on the best estimate of the geometry (design drawings were unavailable) of the coils and the current flowing through the coil was completed. A peak field of about 34 kG was computed at the midpoint of the magnet coils, but the radial magnetic field component was a significant fraction of the axial magnetic field throughout the microwave circuit.

This particular positioning of the coils may have been done to increase the coupling from the beam to the BWO, but at this time the reason for this coil configuration is not understood.

The only parameter not investigated dealt with the repetition rate. The system is presently limited to single shot operation due to cooling of the magnetic field coils, and the ionizing radiation shielding that would be required for the cumulative x-ray dose produced by a very large number (several thousands) of electron beam pulses. However, prior to these measurements repetitive operation with a resistive load and foil diode were completed by UNM (Ref. 4). These tests did demonstrate that the SINUS-VI is capable of 200 Hz operation.

5.0 CONCLUSIONS/RECOMMENDATIONS

The SINUS-VI is comparable to the best systems currently used in U.S. HPM research. While the total radiated power or repetition rate was not observed, the SINUS-VI/BWO system appears to meet the specifications. There are still several research issues which should be addressed in later measurements. They include a simpler antenna which allows analytic calculation of the total rf power. Also, a better understanding of the philosophy behind the nonuniform slow wave structure is needed. That is, what do each of the four radius sections contribute to the overall performance of the nonuniform BWO? Simulations have shown identical power generated in simulations of a BWO as shown in Figure 5 and a BWO composed of the final six periods shown in Figure 5 and a straight cylinder replacing the first five periods (sections A A B B B).* There is a factor of 2 disagreement between the power generated in the experiment and the lower power generated in the simulation. The speculation is that the simulation is not properly handling some aspect of the problem rather than any errors in the measurement of the radiated microwave power. The investigation of the disagreement between simulation and experiment is continuing and will be reported at a later date. The issues of the tapering of the radius, the length of the total structure, and whether sections of the nonuniform BWO act as a prebuncher need to be resolved for an understanding of BWO operation. Also, is it possible to achie.e the same results with a longer electron beam pulse? A fundamental goal of this work is the possible application of the concepts behind this type of HPM device to other types of slow wave HPM sources. Any of these topics would make a suitable engineering or physics doctoral dissertation.

---

*Ray Lemke; SNL, private communication.

REFERENCES

1. Swegle, J.A., Poukey, J.W., and Leifeste, G.T., "Backward Wave Oscillators with rippled wall resonators: Analytic theory and numerical simulation," Phys. Fluids 28(9), pp 2882-2894, September 1985.

2. Korovin, S.D., Polevin, S.D., Roitman, A.M., and Rostov, V.V., "Relativistic Backward Wave tube with variable phase velocity," Sov. Tech. Phys. Lett. 18(4), pp 265-266, April 1992.

3. Korovin, S.D., Bykov, N.M., Gubanov, V.P., Gunin, A.V., Zagulov, F. Ya.,Mesyats, G.A., and Rostov, V.V., "High Current High Repetition Rate Electron Accelerators based on Tesla Transformer," Proc. of the 9th Intnl. Conf. on High-Power Particle Beams, p 481, Washington DC, May 25-29, 1992.

4. Moreland, L., Gahl, J., Shiffler, D., Schamiloglu, E., "Radiated Field Measurements of Repetitively Pulsed, High Power Relativistic Backward Wave Oscillator," Bull. of the American Phys. Soc. 37(6), p 1540, November 1992.

DISTRIBUTION

AFSAA/SAI, Washington, DC
AUL/LSE, Maxwell AFB, AL
DTIC/OCC, Alexandria, VA
PL/HO/SUL/WS/WSR/WSR(HERTF)/
  WST, Kirtland AFB, NM
Sandia National Lab, Albuquerque, NM
Univ of New Mexico, Albuquerque, NM
Official Record Copy
  PL/WSR, Kirtland AFB, NM